doi:10.1093/brain/awh727 *Brain* (2006), **129,** 736–746

Neurophysiological and perceptual correlates of navigational impairment in Alzheimer's disease

Voyko Kavcic, Roberto Fernandez, David Logan and Charles J. Duffy

Departments of Neurology, Brain and Cognitive Sciences, Neurobiology and Anatomy and Ophthalmology and the Center for Visual Science, The University of Rochester Medical Center, Rochester, NY, USA

Correspondence to: Charles J. Duffy, Department of Neurology, University of Rochester Medical Center, 601 Elmwood Avenue, Rochester, New York 14642-0673, USA
E-mail: cjd@cvs.rochester.edu

We assessed visual processing related to navigational impairment in Alzheimer's disease hypothesizing that visual motion evoked responses to optic flow simulating observer self-movement would be linked to navigational performance. Mild Alzheimer's disease and older adult control subjects underwent open-field navigational testing, visual motion perceptual threshold determination and a battery of neuropsychological examinations. We recorded visual motion evoked potentials (EPs) at occipital and parietal sites during centred visual fixation. Randomly moving or stationary pattern pre-stimuli preceded horizontal motion and radial optic flow stimuli to separate motion N200s from pattern onset responses. Radial optic flow evoked N200 responses comparable with those obtained with uniform horizontal motion, despite the variety of motion directions in radial optic flow. Alzheimer's disease patients showed smaller radial optic flow N200s than older adult subjects, and these were greatly diminished when preceded by stationary dots. Combining N200 amplitudes with optic flow perceptual thresholds and contrast sensitivities yielded a strong correlation with navigational impairment in Alzheimer's disease ($R^2 = 0.95$). We conclude that navigational impairment in Alzheimer's disease is linked to a disorder of extrastriate visual cortical motion processing reflected in specific perceptual and neurophysiological measures.

Keywords: Alzheimer's disease; evoked potentials; optic flow; spatial disorientation; navigational impairment

Abbreviations: EPs = evoked potentials; SEM = standard error of measurement

Received September 23, 2005. Revised November 18, 2005. Accepted November 25, 2005; Advance Access publication February 3, 2006

Introduction

Early Alzheimer's disease is characterized by the progressive loss of functional independence that is often linked to visuospatial impairments (Glosser *et al.*, 2002) (Duchek *et al.*, 2003). These deficits commonly occur as part of a syndrome that includes difficulties in both the perceptive and constructive aspects of visuospatial performance and may be the earliest prominent manifestation of Alzheimer's disease in many patients (Cogan, 1985; Becker *et al.*, 1988; Henderson *et al.*, 1989).

Visuospatial processing deficits of cortical origin may play a critical role in the navigational impairments of Alzheimer's disease (Cronin-Golomb *et al.*, 1991; Butter *et al.*, 1996). This may reflect the spread of Alzheimer's pathology into posterior cortical extrastriate visual areas (Brun and Englund, 1981; Benson *et al.*, 1988). In some patients, it may indicate the development of a separate Alzheimer's disease variant with posterior cortical predominance of Alzheimer's pathology (Renner *et al.*, 2004; Tang-Wai *et al.*, 2004).

A variety of basic visual deficits have been described in Alzheimer's disease (Katz and Rimmer, 1989; Gilmore and Levy, 1991) that may reflect more anterior visual mechanisms than those responsible for visual motion processing impairments (Trick and Silverman, 1991; Gilmore *et al.*, 1994; Silverman *et al.*, 1994). Many Alzheimer's disease patients suffer from higher-order visual motion processing deficits (Rizzo and Nawrot, 1998), including selective impairments in perceiving the patterned visual motion of optic flow (Tetewsky and Duffy, 1999) that provides moving observers with information about their heading direction (Gibson, 1950).

Our previous work suggests that Alzheimer's disease patients are unable to access the global patterns of visual

motion in optic flow, forcing them to rely on ambiguous local motion cues (O'Brien *et al.*, 2001). Such higher-order visual processing deficits are correlated with both ambulatory (Tetewsky and Duffy, 1999) and vehicular (O'Brien *et al.*, 2001) navigational impairments in Alzheimer's disease. Visual motion processing deficits may support the early detection of impairment in neuropsychologically intact older adults with a visuospatial form of mild cognitive impairment (Mapstone *et al.*, 2003).

Human visual motion processing can be investigated using scalp-recorded visual motion evoked potentials (EPs) (MacKay and Rietvelt, 1968). A negative wave peaking over parietal areas ~200 ms after stimulus onset (Kuba and Kubova, 1992) is sensitive to the direction and time-course of visual motion stimuli (Bach and Ullrich, 1994). We have now used radial optic flow stimuli to elicit visual motion EPs and have found robust links between EP amplitude, selective impairments of optic flow perception and navigational impairment in Alzheimer's disease patients.

Methods

Subject groups

We studied normal older adult control subjects and Alzheimer's disease patients without ophthalmological or other neuropsychiatric disorders. All subjects had normal, or corrected to normal, visual acuity without group differences by age or gender. Alzheimer's disease subjects were recruited from the clinical programmes of the University of Rochester Alzheimer's Disease Center with probable Alzheimer's disease by National Institutes of Neurological Diseases and Stroke criteria (McKhann *et al.*, 1984). Older adult subjects were recruited from programmes for the healthy elderly or they were the spouses of Alzheimer's disease subjects (Table 1). Informed consent was obtained from all subjects before their enrolment. All procedures were approved by the University of Rochester Medical Center, Research Subjects Review Board.

Subject testing

All tests were administered in the Visual Orientation Laboratory or in the lobby of the Strong Memorial Hospital, Rochester, New York, in two 90 min sessions.

Neuropsychological tests

Neuropsychological tests included the Mini-Mental State Examination (MMSE) (Folstein *et al.*, 1975), which was used in the clinical diagnosis of Alzheimer's disease. The Wechsler Memory Scale-Revised (WMS-R) (Wechsler, 1987) Verbal Paired Associates Test I was used to evaluate immediate and delayed recall for word pairs. Categorical Name Retrieval of animal names was used to test verbal fluency. The Money Road Map test (Money, 1976) was used to evaluate topographical orientation on a route map with subjects using a pencil to trace the route while identifying left and right turns. The WMS-R Figural Memory test was used to evaluate immediate visual recognition. The Judgement of Line Orientation test was used to evaluate the visual processing of simple spatial relations (Benton *et al.*, 1983). Facial Recognition test was used to evaluate the visual processing of complex figures (Benton *et al.*, 1983).

Table 1 Demographics and neuropsychology of subject groups

	Older adult (n = 15)	Alzheimer's disease (n = 15)
Age (years)	70.6 (±9.5)	74.9 (±5.9)
MMSE (max. 30)	28.5 (±1.5)	23.5** (±3.1)
Education (years)	16.2 (±4.4)	14.3 (±2.4)
Money road map (max. 32)	28.1 (±4.3)	24.9* (±4.0)
Figural memory (max. 10)	7.6 (±1.2)	4.6** (±1.1)
Verbal paired assoc. (max. 24)	17.1 (±2.3)	7.5** (±4.2)
Delayed recall (max. 8)	6.5 (±1.1)	3.2** (±2.2)
Verbal fluency (norm. > 12)	22.3 (±4.1)	11.7** (±4.0)
Line orientation (max. 30)	25.1 (±1.9)	20.9* (±5.9)
Facial recognition (max. 54)	46.5 (±3.7)	42.3* (±5.9)
OS (20/x)	37.0 (±22.3)	54.6 (±46.8)
OD (20/x)	39.3 (±44.9)	34.6 (±13.6)
Contrast sensitivity (20/x)	25.7 (±44.9)	37.9* (±17.1)

*P < 0.05, **P < 0.005.

Navigation task

We used a real-world navigation task on a specified route in the Strong Hospital lobby (Fig. 1A inset) as described in a previous publication (Monacelli *et al.*, 2003). Subjects sat in a wheelchair and were instructed to attend to the route as they were pushed along the 1000 ft path over 4 min. We then administered eight tests, each having 10 questions, to assess knowledge of the route, or landmarks along the route, and the integration of route and landmark information.

Several tests were primarily directed at knowledge of the route: *Route Learning:* the route was begun a second time with subjects wheeled to each of 10 choice points and asked whether they had gone left, right or straight at that point. *Self-orientation:* pointing to the direction of pictured scenes from the test route while seated at the starting/finishing point scored as correct if they pointed within 45° of the target. *Route Drawing:* drawing lines on a map of the environment to represent the test route.

Several tests were primarily directed at knowledge of landmarks along the route: *Free Recall:* subjects were given 1 min to name as many objects or landmarks as they could (max. = 10) from the route. *Landmark Recall:* subjects named objects or features (max. = 10) that were helpful in finding their way on the self-directed, second trip around the lobby. *Photograph Recognition:* five photographs of the test path and five from remote public locations in the Medical Center were identified as being from the route or not.

Two tests were primarily directed at the integration of route and landmark knowledge: *Photograph Location*: the viewpoint of 10 photographs from the route was identified by placing an arrow on a route map to indicate the direction from which the picture was taken. *Video Location*: 10 short video clips from the route were presented (PowerPoint, Microsoft Inc., Redmond, WA, USA) and subjects placed an 'x' on a route map where the clip began and an arrow indicating the direction and extent of the depicted movement.

Basic vision

Subjects underwent Snellen visual acuity testing to confirm monocular acuity of at least 20 out of 40. The better eye was used for all subsequent testing that included monocular contrast sensitivity testing at five spatial frequencies from 0.5 to 18 cycles/° (VisTech Inc.,

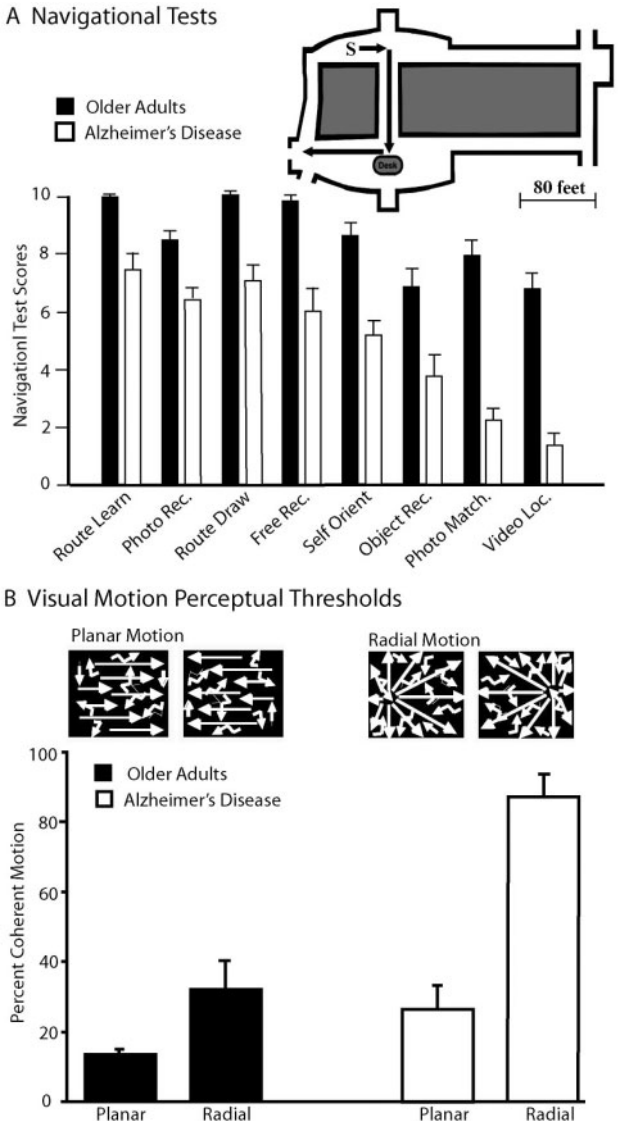

Fig. 1 Test of navigation and visual perception. (**A**) Total and sub-test scores (mean, +1 SEM) from navigational testing of older adult (filled bars) and Alzheimer's disease (open bars) subjects. Alzheimer's disease subjects showed poorer performance with consistently lower scores. Inset shows a survey view of the open-field test environment as an outline of the lobby and the test route. Subjects started and stopped at the location marked by 'S'. Arrows represent 3 of the 10 route segments between decision points. (**B**) Horizontal and radial visual motion combined with varying amounts of random motion were used to determine motion coherence thresholds (mean, +1 SEM) in older adult and Alzheimer's disease subjects. Left- and rightward motions were used to determine a horizontal motion threshold. Inward and outward radial motions were used to determine left/right centre of motion discrimination thresholds. These data yielded significant group × threshold interactions attributable to increased radial thresholds in the Alzheimer's disease group.

Dayton, OH, USA). Contrast sensitivity functions were obtained under the standard lighting conditions required for conversion to equivalent acuity units. All subjects generated CSF curves that satisfied criteria for using this approach (*see* http://www.agingeye.net/cataract/Vistech2.pdf) and yielded contrast sensitivities in the normal range.

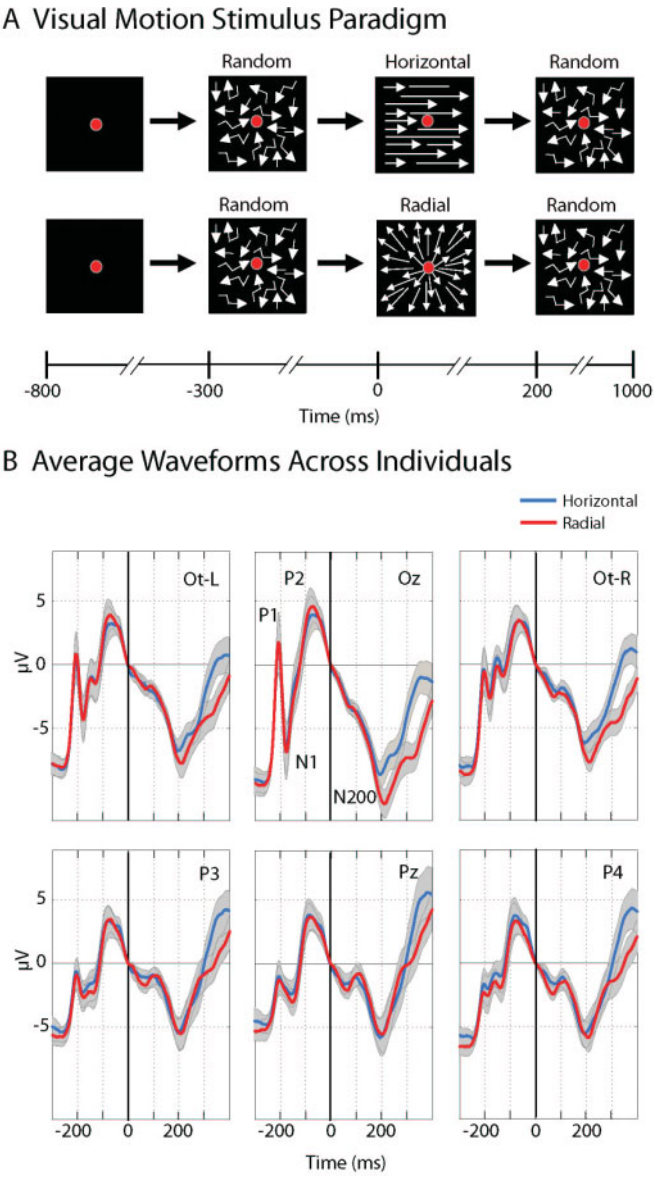

Fig. 2 Horizontal and radial visual motion EPs in older adult subjects. (**A**) Visual motion stimulation paradigms presented random dot motion that transitioned to horizontal or radial motion. (**B**) Averaged waveforms (±1 SEM) for older adult subjects show separate responses to random motion onset and transition to horizontal (blue lines) or radial (red lines) motion. Random motion evoked a visual pattern onset P1, N1, and P2 complex. Despite the assortment of motion directions in radial optic flow, it evoked N200 responses as robust as those seen with horizontal motion.

Psychophysical visual motion stimuli

Subjects underwent psychophysical testing to determine their visual motion coherence thresholds for horizontal and radial (inward/outward) motion using left/right two-alternative forced-choice discrimination (Fig. 2). They sat facing an 8 ft × 6 ft rear-projection tangent screen on which a TV projector (Electrohome, ON, USA) presented animated sequences of 2000 white dots (.13° × .08°, 2.69 cd/m^2) on a dark background over the central 60° × 40° with an average speed of 30°/s at a 60 Hz frame rate.

Horizontal motion stimuli consisted of leftward or rightward moving dots. Radial motion stimuli consisted of dots moving in a radial pattern out from or in to a centre of motion on the horizontal meridian, 20° to the left or right of centre. The horizontal and radial coherent motion patterns were intermixed with random dot motion. The percentage of coherently and randomly moving dots varied between trials for the determination of motion coherence thresholds. Individual dots were randomly assigned to coherent or random motion in each frame. All stimuli had the same dot density, luminance, contrast and average dot speed.

Psychophysical testing paradigm

Motion coherence thresholds were obtained using parameter estimation by sequential testing technique (Pentland, 1980; Harvey, 1997) run initially for 20 trials with a seed value based on pilot data from that subject group (80% coherence for Alzheimer's disease subjects and 50% coherence for young and older normal groups). Each subject's preliminary threshold seeded a subsequent 50-trial run to yield their final threshold. Threshold was the percentage of dots in coherent motion in stimuli *{[coherently moving dots/(coherently moving dots + random dots)] × 100}* yielding 82.5% correct responses, reflecting Weibull fits to psychophysical responses.

Trials began with an audible tone and a centred fixation spot (0.5°). Eye position monitoring by infrared oculometry (ASL) was used to restrict gaze within the central 10°. All subjects maintained stable fixation during testing with few aborted trials. During central fixation, a visual motion stimulus was presented for 1 s and was followed by a pair of audible tones prompting the subject's left or right button press to indicate the direction of horizontal motion or the centre of motion in radial motion within 4 s. Subjects were asked to make their best guess if unsure.

Neurophysiological methods

Neurophysiological visual motion stimuli

Subjects sat in front of a 3 ft × 3 ft rear-projection tangent screen while maintaining centred fixation on a red light-emitting diode (LED) image as monitored by infrared oculography (ASL, Inc., Boston, MA, USA). They viewed a 30° × 30° computer display of 100% coherence horizontal or radial visual motion stimuli while maintaining visual fixation.

Scalp EEG activity was recorded using seven electrode sites chosen to focus on activity in dorsal extrastriate visual cortex. Electrodes were placed according to modified 10–20 system: starting from left occipital-temporal site in counterclockwise order, the OT-L electrode was placed 10% of the Fz-Oz circumference distance from Oz to the left, followed by Oz, OT-R (10% of the Fz-Oz circumference distance from Oz to the right), P4, Pz and P3. We used the Cz electrode as a ground, and two additional electrodes were mounted on the left and right ear lobes for reference. Impedances were maintained below 5 kΩ for each channel and balanced across all channels within a 2 kΩ or less range. EEG was recorded with low- and high-pass filters set at 100 and 0.1 Hz, respectively. The cut-off frequencies for these filters were at 3 dB down and the roll off was 12 dB per octave at both sides. EEG was sampled at 500 Hz per channel with 32-bit resolution. Epochs of approximately 1.5 s duration were collected, and the first 20 ms prior to target presentation was used as a baseline.

Neurophysiological testing paradigm

Visual motion evoked responses were recorded during discrete trials (Fig. 2A). Each trial started with a centred fixation spot; if the subject fixated within 1 s and maintained fixation for an additional 500 ms, the fixation spot was replaced with the pre-stimulus. The pre-stimulus consisted of 1000 single-pixel white dots (as above) displayed at random locations and either remaining stationary or moving randomly. The pre-stimulus was replaced after 300 ms with one of four motion stimuli for 200 ms: left or right horizontally moving dots, or inward or outward radially moving dots. After 200 ms, the pre-stimulus resumed for another 1100 ms, yielding a stimulus duty cycle of 12.5%.

Neurophysiological data analysis

Off-line inspection augmented automatic rejection of EEG epochs contaminated by artefacts before averaging. There were 80–100 repetitions of each condition with <15% rejected trials in all subjects of all groups. Averages were computed for each subject for each electrode and the 10 stimulus conditions: left- and rightward horizontal, in- and outward radial and random dot motion were each recorded after randomly moving and stationary pre-stimuli. Averaged responses plotted with ±1 standard error of measurement (SEM) envelopes were used to identify waveform components. The N200 was identified as peak negative amplitude in the range of 150–300 ms after the motion onset.

Peak amplitudes and latencies of the N200 component relative to motion onset were analysed separately for horizontal (left, right) and radial (in, out) stimuli. Peak N200 amplitudes and latencies from all sites were entered in mixed design ANOVA (analysis of variance) with subject group (older adult, Alzheimer's disease) as a between subjects factor, and site (6) (OT-L, Oz, OT-R, P3, Pz, P4) as a within subjects factor. Greenhouse-Geisser adjustment for the degrees of freedom was used for the recording site factor due to the inherent violations of the repeated measures assumptions of sphericity. Where appropriate, *post hoc* analyses were conducted using Tukey's Honestly Significant Differences (THSD) tests and a family-wise Type I error rate of 0.05.

Neurophysiological measures were combined with psychophysical, neuropsychological and basic visual performance measures in stepwise multiple linear regression analysis (SPSS, 2000). This analysis selected measures that were significant predictors of navigational test scores. The multiple linear regression provided β weights that serve as quantitative assessments of the relative contribution of independent factors to a composite measure correlated with navigational test scores.

Results

Navigation and perception

Older adult and Alzheimer's disease subjects were initially tested on an open-field test of navigational capacity (Monacelli *et al.*, 2003). All subjects were first seated in a wheelchair and passively transported along a standard route in the Strong Hospital lobby (Fig. 1A, top). They then underwent eight tests of navigational capacity, spatial orientation and overall familiarity with that environment (*see* Methods). These tests revealed a range of differences between the two subject groups (Fig. 1A, *bottom*). All tests yielded

significant group effects [MANOVA (multi-way analysis of variance) Hotelling's $T^2_{8,15} = 10.69$, $P < 0.001$] with the largest and most significant differences for the photograph matching [$F(1,22) = 66.93$, $P < 0.001$] and video clip location [$F(1,22) = 57.47$, $P < 0.001$] sub-tests. This replicates our previous findings of substantial navigational impairment in Alzheimer's disease patients compared with older adult subjects (Monacelli *et al.*, 2003). The lowest scores of Alzheimer's disease subjects were on the photo matching and video location sub-tests, suggesting that higher-order visual processing, selectively impaired in Alzheimer's disease, may play a major role in their processing.

We assessed visual processing directly by measuring psychophysical thresholds for visual motion. We determined thresholds for planar (left/right) visual motion and for optic flow, the radial patterns of visual motion that accompany self-movement. The optic flow patterns depicted heading directions 20° to the left or right of centre (Fig. 1B, *top*). Perceptual testing revealed selective elevations of perceptual thresholds for the radial optic flow [interaction $F(1,25) = 16.06$, $P < 0.001$], with *post hoc* THSD identifying higher Alzheimer's disease thresholds for radial motion (Fig. 1B, bottom). Considering the older adult group alone, there is no significant difference between tasks ($t_{12} = 1.92$, $P = 0.08$); for the Alzheimer's disease alone task effect was highly significant ($t_{13} = 6.5$, $P < 0.001$) This replicates our earlier findings of selectively elevated optic flow thresholds in some Alzheimer's disease patients (Tetewsky and Duffy, 1999; O'Brien *et al.*, 2001) and supports the suggestion that these patients have deficits of visual motion processing for spatial orientation.

Optic flow field evoked responses

This combination of navigational and perceptual deficits led us to seek an objective approach to quantifying visual motion processing in Alzheimer's disease patients. We based our efforts on established methods for eliciting visual motion evoked responses (Kuba and Kubova, 1992). Even though radial optic flow contains a mixture of all motion directions that might complicate the neural signature, we reasoned that optic flow response mechanisms that have been identified in monkeys (Duffy and Wurtz, 1995) and humans (O'Craven *et al.*, 1997) might generate specific cortical EPs.

We recorded visual motion EPs by presenting random dot motion 300 ms before the onset of patterned dot motion to distinguish pattern onset and motion onset effects (Fig. 2A). In older adult subjects, horizontal motion stimuli evoke negative deflections peaking at ~180 ms after the onset of patterned motion and are widely distributed across the occipital and parietal leads. Radial optic flow stimuli, interleaved with the horizontal motion trials, elicited averaged N200 responses that tended to be larger at all occipital sites (Fig. 2B).

We derived single-subject averaged N200 response amplitudes to support the statistical comparison of responses to horizontal and radial motion. This approach avoids artefactual amplitude changes from individual differences in peak latency that smear the peak in group averaged waveforms. This analysis revealed a tendency toward a more selective occipital distribution for radial optic flow N200s in older adult subjects, with the largest responses at Oz. However, no significant differences were seen in statistical comparisons of responses to horizontal and radial motion within or between hemispheres.

Thus, radial optic flow evokes N200 responses that are at least as robust as those evoked by horizontal motion. A uniform direction of visual motion is not required to evoke the N200. Rather, the N200 can be evoked by the transition from all directions being combined chaotically in the random motion stimulus to all directions being combined systematically in the radial optic flow stimulus.

Neurophysiology of Alzheimer's disease

We sought neurophysiological links to radial optic flow perceptual impairments in Alzheimer's disease patients by comparing N200 responses between subject groups. Relative to the older adult group, the Alzheimer's disease N200 amplitudes were non-significantly smaller (Fig. 3). The largest difference in peak amplitudes was at Oz [older adult = −9.5 μV, Alzheimer's disease = −7.6 μV, group $F(1,27) = 2.40$, $P = 0.13$] and was accompanied by a non-significant delay [older adult = −221 ms, Alzheimer's disease = −225 ms, group $F(1,27) = 0.39$, $P = 0.54$] (Fig. 5, blue circles). Groupwise analyses of the horizontal motion N200 responses yielded similar results for amplitudes ($P = 0.10$) and latencies ($P = 0.55$).

To better simulate the abrupt onsets and halts that characterize the episodic nature of active self-movement, we used stimuli in which stationary dots preceded the radial optic flow (Fig. 4A). The stationary-to-radial N200 responses yielded large group differences that were not seen with the random-to-radial transition (Fig. 4B). Relative to the older adult, the Alzheimer's disease N200 amplitudes were significantly smaller [Oz: older adult = −8.3 μV, Alzheimer's disease = −3.6 μV, group $F(1,28) = 13.69$, $P = 0.001$] (Fig. 5, red circles). Comparable analyses of horizontal motion N200 responses also showed significantly smaller amplitudes in the Alzheimer's disease group [Oz: older adult = −6.8 μV, Alzheimer's disease = −3.3 μV, group $F(1,28) = 5.91$, $P = 0.02$] without significant latency differences ($P = 0.33$).

Single-subject N200 response amplitudes were again used for the statistical comparison of subject groups, avoiding artefactual amplitude changes from individual differences in peak latency. Older adult and Alzheimer's disease subjects showed different effects of random motion versus stationary pre-stimuli on their N200 responses to radial optic flow.

In older adult subjects, random-to-radial N200s were more prominent in the occipital leads, whereas stationary-to-radial N200s were uniformly large across all occipital and parietal leads [pre-stimulus X site interaction effects, $F(1,3) = 9.54$, $P < 0.001$]. This interaction effect was attributable to larger

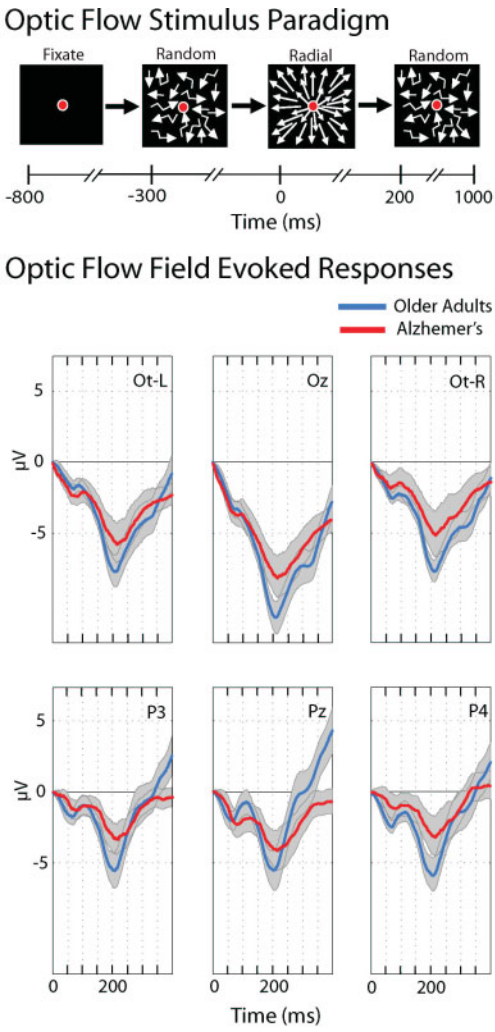

Fig. 3 Random motion to radial optic flow EPs in older adult and Alzheimer's disease subjects. (**A**) Random motion preceded radial optic flow stimulation. (**B**) Averaged waveforms (±1 SEM) for older adult (blue lines) and Alzheimer's disease (red lines) subjects showed robust N200 responses. There is a non-significant trend toward smaller responses in the Alzheimer's disease group ($P = 0.30$) without significant subject group by recording site interactions ($P = 0.23$).

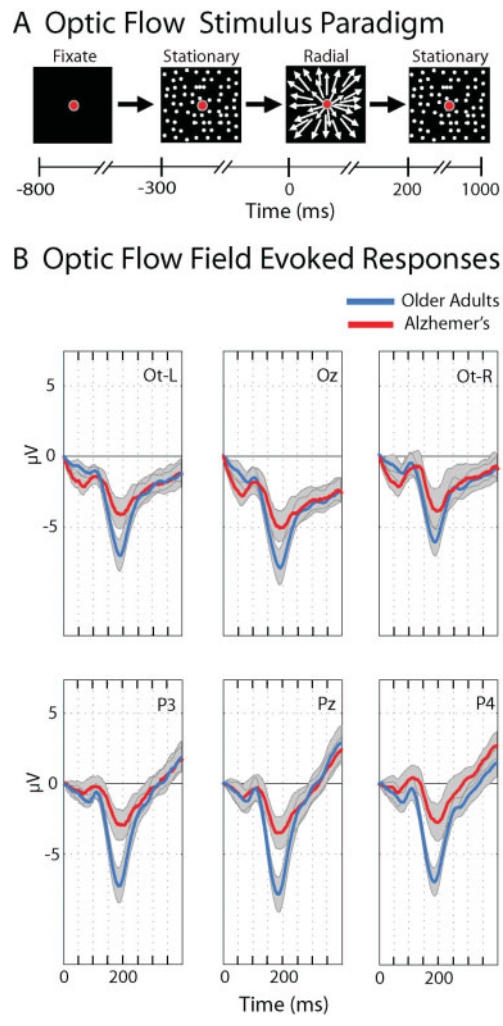

Fig. 4 Stationary dots to radial optic flow evoked responses in older adult and Alzheimer's disease subjects. (**A**) Stationary dots preceded radial optic flow stimulation. (**B**) Averaged waveforms (±1 SEM) showed much larger N200 responses for older adult subjects (blue lines) than for Alzheimer's disease subjects (red lines), especially at parietal sites.

radial N200s in the parietal leads after stationary pre-stimuli (THSD, $P < 0.001$). (Fig. 5A).

In Alzheimer's disease subjects, random-to-radial N200s showed the same pattern of occipital predominance seen in older adult subjects (Fig. 5, blue circles). Unlike older adult subjects, the Alzheimer's disease patients showed uniformly small stationary-to-radial N200s across all occipital and parietal leads [pre-stimulus × site interaction effects, $F(1,5) = 9.22$, $P < 0.001$]. This interaction effect was attributable to larger radial N200s in the occipital leads after random pre-stimuli (THSD, $P < 0.001$) (Fig. 5B, blue circles).

Thus, random-to-radial transitions evoke only subtle differences in the occipitally predominant N200s of older adult and Alzheimer's disease subjects; Alzheimer's disease subjects do not generally have greatly diminished N200s. However, stationary-to-radial transitions evoke substantial N200s only in older adult subjects, with greatly diminished N200 responses in Alzheimer's disease patients only under those conditions.

Navigational mechanisms in Alzheimer's disease

The robust N200s evoked by radial optic flow, and their sensitivity to preceding visual stimuli, suggested that they may be an important source of information about visual processing impairments in Alzheimer's disease. We tested this hypothesis by developing a linear regression model of navigational performance that combines neuropsychological, neurophysiological and psychophysical characterizations of older adult and Alzheimer's disease subjects.

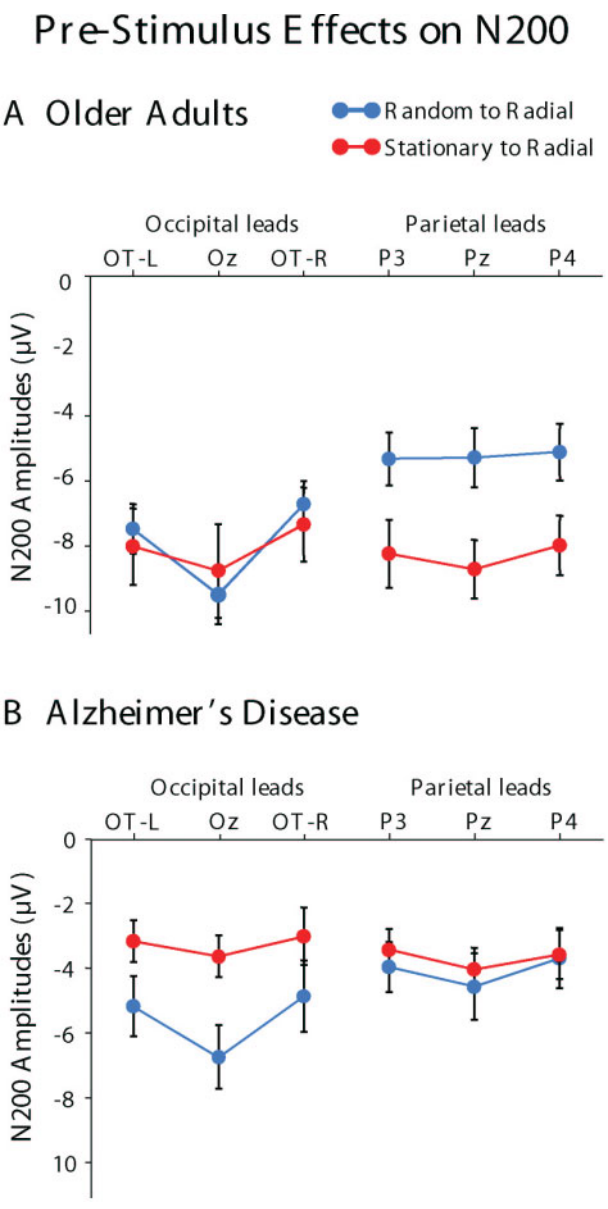

Fig. 5 Averaged single-subject peak responses (±1 SEM) for older adult and Alzheimer's disease subjects when random motion preceded radial motion (blue lines) or stationary dots preceded radial motion (red lines). (**A**) In older adult subjects, random motion pre-stimuli yielded large N200 responses that were larger at occipital sites and substantially smaller at parietal sites. (Note that larger N200 responses are plotted further down along the negative ordinate scale.) Stationary-to-radial transitions evoked uniformly large N200s across all sites in older adult subjects. (**B**) In Alzheimer's disease subjects, random motion pre-stimuli yielded somewhat smaller N200 responses than seen in older adult subject. The N200 responses of Alzheimer's disease subjects were again larger at occipital sites and smaller at parietal sites. Stationary-to-radial transitions evoked uniformly small N200s across all sites in Alzheimer's disease subjects.

We used the radial optic flow N200 amplitudes and latencies of each subject, in occipital and parietal leads, with random and stationary pre-stimuli, as measures of cortical responsiveness to optic flow. These were combined with the horizontal motion and radial optic flow coherence thresholds, and the difference between those thresholds, as measures of optic flow discrimination. We included neuropsychological test scores as measures of cognitive capacity and basic visual test scores as measures of sensory capacity (Table 1) using data from the 23 subjects (older adult = 12, Alzheimer's disease = 11) who completed all aspects of all of the studies.

Table 2 Standardized regression coefficients for stepwise regression analysis

Variables	β	Significance
Difference of thresholds	−0.713	<0.0005
N200 amplitude at Oz	−0.378	<0.0005
Contrast sensitivity	−0.191	0.006
Line orientation	−0.115	0.060
Money road map	−0.070	0.219
Snellen acuity	−0.061	0.298
Figural memory	−0.077	0.332
Facial recognition	−0.043	0.503
Verbal fluency	0.043	0.589
Delayed recall	0.005	0.942
Radial motion threshold	0.003	0.958
Verbal paired assoc.	0.001	0.989

Multiple linear regression analysis selected three variables as being linked to navigational tests scores: the difference between horizontal and radial thresholds, the stationary-to-radial N200 amplitudes at Oz and contrast sensitivities (Table 2). These variables yielded a strong correlation with navigational performance [R^2_{adj} = 0.95; $F(3,20)$ = 131.4, $P < 0.001$] (Fig. 6). The threshold differences, N200 amplitudes and contrasts were separate and substantial contributors to the navigational test scores with highly significant beta weights in the resulting model ($\beta_{thresholds}$ = 0.71, $P < 0.001$; β_{N200} = 0.38, $P < 0.001$; $\beta_{contrast}$ = 0.19, P = 0.006). All of the other variables were excluded by the analysis, as were two very impaired Alzheimer's disease subjects who were identified as outliers and were consequently removed from the analysis.

These findings link navigational capacities with psychophysical, neurophysiological and basic visual measures of optic flow analysis. The unique contribution of each of these measures suggests that they reflect separate aspects of navigational impairment in Alzheimer's disease.

Discussion

Navigation and perception in Alzheimer's disease

Our Alzheimer's disease patients showed broad-based impairments in a naturalistic test of navigational capacity. The largest differences with older adult subjects were measured by sub-tests that require identifying the location along the test route that corresponds to a photographically or videographi-

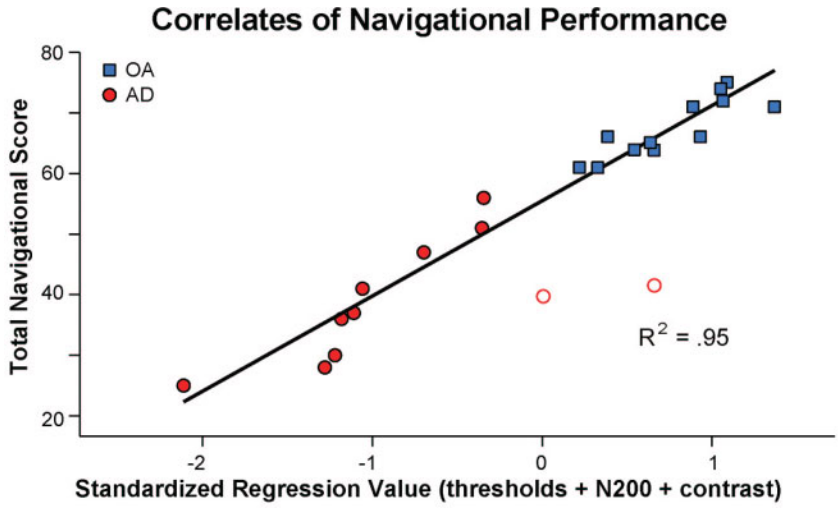

Fig. 6 Perceptual and neurophysiological correlates of navigational impairment. Scatter plot of total navigational test score (ordinate) by composite multiple linear regression predictor (abscissa) for all older adult (blue squares) and Alzheimer's disease (red circles) subjects. Stepwise regression selected the difference between horizontal and radial thresholds (β = 0.71), the stationary-to-radial N200 response amplitude (β = 0.38) and visual contrast sensitivity (β = 0.19) as significant predictors to yield a composite R^2 = 0.95. The regression analysis rejected the inclusion of the other neuropsychological, perceptual and neurophysiological variables. The analysis identified two Alzheimer's disease subjects as being very impaired outliers (open red circles).

cally displayed scene from the route (Fig. 1A). All Alzheimer's disease subjects scored better on the tests of route and location knowledge, suggesting particular impairment of the ability to link those types of navigational information into an integrated cognitive map of the environment (Golledge, 1999; Redish, 1999). These navigational studies also confirm our findings from an earlier series of Alzheimer's disease patients that linked those sub-tests to older adult and Alzheimer's disease subjects becoming lost in the test environment (Monacelli *et al.*, 2003). Such results are consistent with the proposal that navigational impairments in Alzheimer's disease primarily reflect cortical visual processing deficits (Cogan, 1985; Benson *et al.*, 1988; Cronin-Golomb *et al.*, 1991). This is supported by the selective elevation of radial optic flow motion coherence thresholds in the Alzheimer's disease group (Fig. 1B) much as we described in our earlier studies (Tetewsky and Duffy, 1999; O'Brien *et al.*, 2001).

The first quantitative characterizations of visual impairments in Alzheimer's disease focused on links between disease severity and contrast sensitivity deficits (Gilmore and Levy, 1991). Later work demonstrated that horizontal motion thresholds increase linearly with ageing but with significant differences between Alzheimer's disease patients and age-matched controls (Trick and Silverman, 1991). These deficits were found to be independent of contrast sensitivity impairments, implying a central origin (Gilmore *et al.*, 1994). Preserved motion detection thresholds, in the setting of elevated motion discrimination thresholds, suggested an underlying intra-cortical disconnection in a hierarchically organized visual motion processing stream (Silverman *et al.*, 1994). This interpretation was consistent with the finding that Alzheimer's disease particularly affects cortico-cortical projection neurons (Hof *et al.*, 1990).

We applied the disconnection model of central processing deficits in Alzheimer's disease to explain the agnosia for simulated heading direction in optic flow observed in the setting of preserved optic flow coherence thresholds (Tetewsky and Duffy, 1999). Cortico-cortical disconnection in Alzheimer's disease (Morrison *et al.*, 1991) may also underlie the failure of large-scale spatial integration required to process the global pattern of visual motion in optic flow. This forces Alzheimer's disease patients to rely on local motion cues (O'Brien *et al.*, 2001) that expose the earliest signs of such deficits in mild cognitive impairment (Mapstone *et al.*, 2003). The implied limit on the spatial range of visual integration supports the idea that cortico-cortical interactions for the integration of motion signals may be critically involved in the visual deficits of Alzheimer's disease.

Neurophysiology of visual motion processing in Alzheimer's disease

Alzheimer's disease has been associated with increased latencies of pattern shift visual EPs (Coben *et al.*, 1983; Pollock *et al.*, 1989), particularly affecting later components (N140, P200) (Philpot *et al.*, 1990; Martinelli *et al.*, 1996). These effects may distinguish Alzheimer's disease from other dementias, psychiatric illness and healthy older adults (Moore *et al.*, 1996) or even identify a subgroup of Alzheimer's disease patients with prominent visuospatial impairments (Swanwick *et al.*, 1996), but their utility as a diagnostic tool is limited (Coburn *et al.*, 2003). Delayed visual evoked responses may reflect the posterior cortical hypometabolism (Pietrini *et al.*, 1996) and atrophy (Hof *et al.*, 1997) associated with visual impairment in Alzheimer's disease.

We developed cortical evoked response measures of radial optic flow analysis on the basis of earlier descriptions of N200 evoked responses to horizontal visual motion in young, healthy subjects (Kubova *et al.*, 1995; Niedeggen and Wist, 1998). Our studies demonstrate that radial optic flow can evoke large occipital responses (Fig. 2B) even though the radial pattern contains all the same directions of motion as the preceding random motion. Thus, the random-to-radial transition can serve as a measure of specific responses to the patterned motion of radial optic flow.

We used stationary-to-radial transitions as a more naturalistic stimulus that includes the visual transitions simulated from a stationary position to movement expected when navigating through the environment. Stationary-to-radial transitions evoked more broadly distributed responses in older adult subjects with high-amplitude N200s in both occipital and parietal leads (Fig. 5A). This may reflect the large number of posterior occipital and parietal cortical areas activated by the onset of visual motion (Orban and Vanduffel, 2004). In contrast, the same stationary-to-radial transition evokes no substantial N200 response in Alzheimer's disease subjects at occipital or parietal sites (Fig. 5B).

The absence of radial N200s after stationary pre-stimuli in Alzheimer's disease may relate to their inability to perceive target stimuli imbedded in a rapid serial presentation with distractor stimuli, that is, the attentional blink (Raymond, 2000). Prolonged attentional blinks are correlated with elevated optic flow perceptual thresholds in Alzheimer's disease (Kavcic and Duffy, 2003), possibly because inhibitory mechanisms block the early processing of new stimuli during the prolonged periods required for subsequent signal processing in Alzheimer's disease (Chun and Potter, 1995; Kavcic and Duffy, 2003).

Alternatively, the absence of radial N200s after stationary pre-stimuli in Alzheimer's disease may reflect an additive effect of local and global processing mechanisms. Random and radial motion have the same diverse set of local motion directions, so the random-to-radial transition activates only global motion mechanisms yielding smaller N200s in Alzheimer's disease. Stationary and radial stimuli differ with respect to both local and global motion, so the stationary-to-radial transition reflects the cumulative effect of Alzheimer's disease on both local and global motion processing. The involvement of local processing mechanisms in the motion response impairment of Alzheimer's disease is supported by the finding of significant decrements in the static-to-horizontal transitions.

Neither the random nor the stationary pre-stimuli evoked the hemispheric lateralization of visual motion N200s seen in previous studies (Niedeggen and Wist, 1999; Hollants-Gilhuijs *et al.*, 2000). This may be the result of the large screen stimuli used in our laboratory to simulate the self-movement scene. The effect of stimulus size might be mediated by the extensive callosal connections of dorsal extrastriate areas (Maunsell and Essen, 1987), including those areas that are specialized for optic flow analysis (Duffy and Wurtz, 1991; Orban *et al.*, 1992; Graziano *et al.*, 1994) related to self-movement perception (Duffy and Wurtz, 1995; Lappe, 1996; Britten and Van Wezel, 1998) and navigation (Froehler and Duffy, 2002).

Visual mechanisms of navigational impairment in Alzheimer's disease

We developed a regression model that linked navigational impairment in Alzheimer's disease to the difference between horizontal and radial motion coherence thresholds, radial N200 amplitudes at Oz and contrast sensitivities (Table 2, Fig. 6). This model ranked the difference in perceptual thresholds as the strongest factor, followed by N200 amplitudes and contrast sensitivities. These three regressors were highly significant, independent of each other and combined to explain 95% of the variance in navigational performance. All other measures were non-significant in the context of these three regressors as reflected by higher *P*-values and lower β weights for next closest regressors from the line orientation and road map neuropsychological tests. As in our previous studies (O'Brien *et al.*, 2001; Mapstone *et al.*, 2003), the memory impairment that is an important aspect of disability in Alzheimer's disease was not related strongly to navigational capacity.

The correlative links between visual processing measures and navigational capacity do not prove direct causal relations; some other factor could possibly mediate both effects. Nevertheless, we can consider that the relative contributions of the three visual factors identified as significant regressors may reflect deficits distributed across stages in the hierarchy of dorsal extrastriate processing for navigation. Visual motion thresholds reflect self-movement direction discrimination, a capacity that is commonly attributed to posterior parietal areas (Critchley, 1953; Mountcastle *et al.*, 1975); by controlling for the basic visual attributes of the stimuli that are shared by both horizontal and radial motion. N200 amplitudes might provide a more direct measure of occipitoparietal visual motion processing for self-movement analysis (Duffy, 1998; Nakamura, 1999). Finally, contrast sensitivity may relate to visual detection mediated by retino-geniculo-calcarine processing (Keri *et al.*, 1999; Crow *et al.*, 2003), apparently suggesting that the threshold differences could not entirely account for differences in basic visual capacities. These three independent factors might reflect components of a serial processing stream in a hierarchical model of visual processing for navigation. Serial hierarchical models are consistent with a multi-factorial view of visuospatial impairment in Alzheimer's disease and the sequential extension of Alzheimer's disease pathology throughout the visual system (Hof *et al.*, 1997; Wong-Riley *et al.*,1997).

Our findings demonstrate a link between measures of navigational impairment (Monacelli *et al.*, 2003) and selective deficits in related perceptual capacities in early Alzheimer's disease (O'Brien *et al.*, 2001). These studies illustrate the utility of neurophysiological measures in assessing specific aspects of cortical information processing. The combination

of psychophysical and neurophysiological methods may contribute to the quantitative characterization of impairment with important implications for evaluating functional capacities.

Acknowledgements

We thank Drs Laura Cushman, Mark Mapstone and William K. Page, as well as Sarita Kishore, William Vaughn and Teresa Steffenella for comments on an earlier draft of the manuscript. We gratefully acknowledge William Vaughn's expertise in the development of the software used in these studies. We are also grateful for Teresa Steffenella's contributions to all of these experiments. This work was supported by grants from NIA (AG17596), NEI (EY10287) and the Alzheimer's Association (IIRG001977) to CJD.

References

Bach M, Ullrich D. Motion adaptation governs the shape of motion-evoked cortical potentials. Vision Res 1994; 34: 1541–7.

Becker JT, Huff FJ, Nebes RD, Holland A, Boller F. Neuropsychological function in Alzheimer's disease: pattern of impairment and rates of progression. Arch Neurol 1988; 45: 263–8.

Benson DF, Davis RJ, Snyder BD. Posterior cortical atrophy. Arch Neurol 1988; 45: 789–93.

Benton A, Hamsher K, Varney NR, Spreen O. Contributions to neuropsychological assessment: a clinical manual. New York: Oxford University Press; 1983.

Britten KH, Van Wezel RJ. Electrical microstimulation of cortical area MST biases heading perception in monkeys. Nat Neurosci 1998; 1: 59–63.

Brun A, Englund E. Regional pattern of degeneration in Alzheimer's disease: neuronal loss and histopathological grading. Histopathology 1981; 5: 549–64.

Butter CM, Trobe JD, Foster NL, Brent S. Visual-spatial deficits explain visual symptoms in Alzheimer's disease. Am J Ophthalmol 1996; 122: 97–105.

Chun MM, Potter MC. A two-stage model for multiple target detection in rapid serial visual presentation. J Exp Psychol 1995; 21: 109–27.

Coben LA, Danziger WL, Hughes CP. Visual evoked potentials in mild senile dementia of Alzheimer type. Electroencephalogr Clin Neurophysiol 1983; 55: 121–30.

Coburn KL, Arruda JE, Estes KM, Amoss RT. Diagnostic utility of visual evoked potential changes in Alzheimer's disease. J Neuropsychiatry Clin Neurosci 2003; 15: 175–9.

Cogan DG. Visual disturbances with focal progressive dementing disease. Am J Ophthalmol 1985; 100: 68–72.

Critchley M. The parietal lobes. New York: Hafner Publishing Co.; 1953.

Cronin-Golomb A, Corkin S, Rizzo JF, Cohen J, Growdon JH, Banks KS. Visual dysfunction in Alzheimer's disease relation to normal aging. Ann Neurol 1991; 29: 41–52.

Crow RW, Levin LB, LaBree L, Rubin R, Feldon SE. Sweep visual evoked potential evaluation of contrast sensitivity in Alzheimer's dementia. Invest Ophthalmol Vis Sci 2003; 44: 875–8.

Duchek JM, Carr DB, Hunt L, Roe CM, Xiong C, Shah K et al. Longitudinal driving performance in early-stage dementia of the Alzheimer type. J Am Geriatr Soc 2003; 51: 1342–7.

Duffy CJ. MST neurons respond to optic flow and translational movement. J Neurophysiol 1998; 80: 1816–27.

Duffy CJ, Wurtz RH. Sensitivity of MST neurons to optic flow stimuli. I. A continuum of response selectivity to large-field stimuli. J Neurophysiol 1991; 65: 1329–45.

Duffy CJ, Wurtz RH. Response of monkey MST neurons to optic flow stimuli with shifted centers of motion. J Neurosci 1995; 15: 5192–208.

Folstein MF, Folstein SE, McHugh PR. 'Mini-mental state'. A practical method for grading the cognitive state of patients for the clinician. J Psychiatric Res 1975; 12: 189–98.

Froehler MT, Duffy CJ. Cortical neurons encoding path and place: where you go is where you are. Science 2002; 295: 2462–5.

Gibson JJ. The perception of the visual world. Boston, MA: Houghton Mifflin; 1950.

Gilmore GC, Levy JA. Spatial contrast sensitivity in Alzheimer's disease: a comparison of two methods. Optom Vis Sci 1991; 68: 790–4.

Gilmore GC, Wenk HE, Naylor LA, Koss E. Motion perception and Alzheimer's disease. J Gerontol 1994; 49: P52–7.

Glosser G, Gallo J, Duda N, de V, Clark CM, Grossman M. Visual perceptual functions predict instrumental activities of daily living in patients with dementia. Neuropsychiatry Neuropsychol Behav Neurol 2002; 15: 198–206.

Golledge RG. Wayfinding behavior: cognitive mapping and other spatial processes. Baltimore, MD: The Johns Hopkins University Press; 1999.

Graziano MSA, Andersen RA, Snowden RJ. Tuning of MST neurons to spiral motion. J Neurosci 1994; 14: 54–67.

Harvey LO. Efficient estimation of sensory thresholds with ML-PEST. Spat Vis 1997; 11: 121–8.

Henderson VW, Mack W, Williams BW. Spatial disorientation in Alzheimer's disease. Arch Neurol 1989; 46: 391–4.

Hof PR, Bouras C, Constantinidis J, Morrison JH. Selective disconnection of specific visual association pathways in cases of Alzheimer's disease presenting with Balint's syndrome. J Neuropathol Exp Neurol 1990; 49: 168–84.

Hof PR, Vogt BA, Bouras C, Morrison JH. Atypical form of Alzheimer's disease with prominent posterior cortical atrophy: a review of lesion distribution and circuit disconnection in cortical visual pathways. Vision Res 1997; 37: 3609–25.

Hollants-Gilhuijs MA, de Munck JC, Kubova Z, van Royen E, Spekreijse H. The development of hemispheric asymmetry in human motion VEPs. Vision Res 2000; 40: 1–11.

Katz B, Rimmer S. Ophthalmologic manifestations of Alzheimer's disease. Surv Ophthalmol 1989; 34: 31–43.

motion-onset and pattern-reversal evoked potentials. Vision Res 1995; 35: 197–205.

Lappe M. Functional consequences of an integration of motion and stereopsis in area MT of monkey extrastriate visual cortex. Neural Comput 1996; 8: 1449–61.

MacKay DM, Rietvelt WJ. Electroencephalogram potential evoked by accelerated visual motion. Nature 1968; 217: 677–8.

Mapstone M, Steffenella TM, Duffy CJ. A visuospatial variant of mild cognitive impairment: getting lost between aging and AD. Neurology 2003; 60: 802–8.

Martinelli V, Locatelli T, Comi G, Lia, C, Alberoni M, Bressi S et al. Pattern visual evoked potential mapping in Alzheimer's disease: correlations with visuospatial impairment. Dementia 1996; 7: 63–8.

Maunsell JHR, Van Essen DC. Topographic organization of the middle temporal visual area in the macaque monkey: representational bias and the relationship to callosal connections and myeloarchitectonic boundaries. J Comp Neurol 1987; 266: 535–5.

McKhann G, Drachman D, Folstein M, Katzman R, Price D, Stadlan EM. Clinical diagnosis of Alzheimer's disease: report of the NINCDS-ADRDA Work Group under the auspices of Department of Health and Human Services Task Force on Alzheimer's Disease. Neurology 1984; 34: 939–44.

Monacelli AM, Cushman LA, Kavcic V, Duffy CJ. Spatial disorientation in Alzheimer's disease: the remembrance of things passed. Neurology 2003; 61: 1491–7.

Money J. A Standardized road map test of direction sense. San Rafael, CA: Academic Therapy Publications; 1976.

Moore NC, Vogel RL, Tucker KA, Khairy NM, Coburn KL. P2 flash visual evoked response delay may be a marker of cognitive dysfunction in healthy elderly volunteers. Int Psychogeriatr 1996; 8: 549–59.

Morrison JH, Hof PR, Bouras C. An anatomic substrate for visual disconnection in Alzheimer's disease. Ann N Y Acad Sci 1991; 640: 36–43.

Mountcastle VB, Lynch JC, Georgopoulos AP, Sakata H, Acuna C. Posterior parietal association cortex of the monkey: command functions for operations within extrapersonal space. J Neurophysiol 1975; 38: 871–908.

Nakamura JOK. Topographical analysis of motion-triggered visual evoked potentials in man. Jpn J Ophthalmol 1999; 43: 36–43.

Niedeggen M, Wist ER. Motion evoked brain potentials parallel the consistency of coherent motion perception in humans. Neurosci Lett 1998; 246: 61–4.

Niedeggen M, Wist ER. Characteristics of visual evoked potentials generated by motion coherence onset. Brain Res Cogn Brain Res 1999; 8: 95–105.

O'Brien HL, Tetewsky S, Avery LM, Cushman LA, Makous W, Duffy CJ. Visual mechanisms of spatial disorientation in Alzheimer's disease. Cereb Cortex 2001; 11: 1083–92.

O'Craven KM, Rosen BR, Kwong KK, Treisman A, Savoy RL. Voluntary attention modulates fMRI activity in human MT-MST. Neuron 1997; 18: 591–8.

Orban GA, Lagae L, Verri A et al. First-order analysis of optical flow in monkey brain. Proc Natl Acad Sci USA 1992; 89: 2595–99.

Orban GA, Vanduffel W. Functional mapping of motion regions. In: Chalupa LM, Werner JS, editors. The visual neurosciences. Cambridge: MIT Press; 2004. p. 1229–46.

Pentland A. Maximum likelihood estimation: the best PEST. Percept Psychophys 1980; 28: 377–9.

Philpot MP, Amin D, Levy R. Visual evoked potentials in Alzheimer's disease: correlations with age and severity. Electroencephalogr Clin Neurophysiol 1990; 77: 323–29.

Pietrini P, Furey ML, Graff-Radford N et al. Preferential metabolic involvement of visual cortical areas in a subtype of Alzheimer's disease: clinical implications. Am J Psychiatry 1996; 153: 1261–68.

Pollock VE, Schneider LS, Chui HC, Henderson V, Zemansky M, Sloane RB. Visual evoked potentials in dementia: a meta-analysis and empirical study of Alzheimer's disease patients. Biol Psychiatry 1989; 25: 1003–13.

Raymond JE. Attentional modulation of visual motion perception. Trends Cogn Sci 2000; 4: 42–50.

Redish AD. Beyond the cognitive map: from place cells to episodic memory. Cambridge: MIT Press; 1999.

Renner JA, Burns JM, Hou CE, McKeel DW, Storandt M, Morris JC. Progressive posterior cortical dysfunction: a clinicopathologic series. Neurology 2004; 63: 1175–80.

Rizzo M, Nawrot M. Perception of movement and shape in Alzheimer's disease. Brain 1998; 121: 2259–70.

Silverman SE, Tran DB, Zimmerman KM, Feldon SE. Dissociation between the detection and perception of motion in Alzheimer's disease. Neurology 1994; 44: 1814–18.

SPSS I. SPSS v10. Upper Saddle River, NJ: Prentice Hall; 2000.

Swanwick GR, Rowan M, Coen RF et al. Clinical application of electrophysiological markers in the differential diagnosis of depression and very mild Alzheimer's disease. J Neurol Neurosurg Psychiatry 1996; 60: 82–6.

Tang-Wai DF, Graff-Radford NR, Boeve BF, Dickson DW, Parisi JE, Crook R et al. Clinical, genetic, and neuropathological characteristics of posterior cortical atrophy. Neurology 2004; 63: 1168–74.

Tetewsky S, Duffy CJ. Visual loss and getting lost in Alzheimer's disease. Neurology 1999; 52: 958–65.

Trick GL, Silverman SE. Visual sensitivity to motion: age-related changes and deficits in senile dementia of the Alzheimer type. Neurology 1991; 41: 1437–40.

Wechsler D. Wechsler Memory Scale, Revised Manual. San Antonio, TX: Psychological Corporation; 1987.

Wong-Riley M, Antuono P, Ho KC. Cytochrome oxidase in Alzheimer's disease: biohemical, histochemical, and immunohistochemical analyses of the visual and other systems. Vision Res 1997; 37: 3593–608.